Inhibition of ATPase, GTPase and adenylate kinase activities of the second nucleotide-binding fold of the cystic fibrosis transmembrane conductance regulator by genistein

Christoph RANDAK*[1], Ennes A. AUERSWALD†, Irmgard ASSFALG-MACHLEIDT‡, William W. REENSTRA§ and Werner MACHLEIDT‡

*Kinderklinik im Dr. von Haunerschen Kinderspital, Ludwig-Maximilians-Universität München, Lindwurmstrasse 4, D-80337 München, Germany, †Abteilung für Klinische Chemie und Klinische Biochemie der Chirurgischen Klinik und Poliklinik, Klinikum Innenstadt der Ludwig-Maximilians-Universität München, Nussbaumstrasse 20, D-80336 München, Germany, ‡Institut für Physiologische Chemie, Physikalische Biochemie und Zellbiologie, Ludwig-Maximilians-Universität München, Goethestrasse 20, D-80336 München, Germany, and §Departments of Clinical Science and Pediatrics, Alfred I. duPont Hospital for Children, Thomas Jefferson University, Wilmington, DE 19803, U.S.A.

In the presence of ATP, genistein, like the ATP analogue adenosine 5′-[β,γ-imido]triphosphate (pp[NH]pA), increases cystic fibrosis transmembrane conductance regulator (CFTR) chloride currents by prolonging open times. As pp[NH]pA is thought to increase CFTR currents by interfering with ATP hydrolysis at the second nucleotide-binding fold (NBF-2), the present study was undertaken to investigate the effects of genistein on a fusion protein comprising maltose-binding protein (MBP) and NBF-2 (MBP–NBF-2). MBP–NBF-2 exhibited ATPase, GTPase and adenylate kinase activities that were inhibited by genistein in a partial non-competitive manner with respect to ATP or GTP. K_i values for competitive and uncompetitive inhibition were respectively 20 μM and 63 μM for ATPase, 15 μM and 54 μM for GTPase, and 46 μM and 142 μM for adenylate kinase. For ATPase activity, genistein reduced V_{max} by 29 % and V_{max}/K_m by 77 %. Additional evidence for complex-formation between genistein and MBP–NBF-2 was obtained by the detection of genistein-dependent alterations in the CD spectrum of MBP–NBF-2 that were consistent with the formation of a higher-ordered state. Addition of MBP–NBF-2 increased the fluorescence intensity of genistein, consistent with a change to a less polar environment. pp[NH]pA partially eliminated this enhanced fluorescence of genistein. These observations provide the first direct biochemical evidence that genistein interacts with CFTR, thus inhibiting NBF-2 activity, and suggest a similar mechanism for genistein-dependent stimulation of CFTR chloride currents.

Key words: CD, enzyme inhibitors, fluorescence, isoflavones, kinetics.

INTRODUCTION

The cystic fibrosis transmembrane conductance regulator (CFTR) is a chloride channel that has been predicted to contain two nucleotide-binding folds (NBF-1 and NBF-2) [1] with sequence identity with other NBFs of the ATP-binding cassette family, with adenylate kinase and with heterotrimeric G-proteins [1–3]. CFTR channel gating requires both phosphorylation by cAMP-dependent protein kinases [4] and the presence of cytosolic hydrolysable nucleoside triphosphates [5]. Previous electrophysiological studies have established a preliminary model in which the interaction of ATP with both NBFs controls channel opening [6–8], while ATP hydrolysis at NBF-2 controls channel closing [7–9]. We have shown that a recombinant CFTR NBF-2 protein possessed two distinct nucleotide-binding sites, one for ATP and GTP [10,11] and one for AMP [10,12]. Both ATP and GTP were substrates for hydrolysis and, in the presence of AMP, the ATPase reaction was replaced by the formation of two ADP molecules from ATP and AMP. In contrast with the action of several other adenylate kinases, including that from *Escherichia coli* [13,14], the transfer of a phosphoryl group from GTP to AMP was not catalysed [12].

Genistein (4′,5,7-trihydroxyisoflavone) is an isoflavonoid that inhibits several ATP-binding enzymes, such as protein tyrosine kinases [15] and protein histidine kinase [16]. Genistein has been shown to activate CFTR Cl^- channels in a variety of cells, including human airway epithelia [17–21], as well as in the most common disease-associated mutant CFTR, i.e. CFTRΔF508 (CFTR lacking Phe-508) [22]. Original studies had proposed an influence of genistein on a cAMP-independent regulatory pathway that possibly involves inhibitory tyrosine phosphorylation [17,18]. Subsequent studies suggested that genistein activates CFTR via inhibition of CFTR dephosphorylation [19,23,24]. Evidence supporting this latter theory includes the observations that genistein increases the steady-state phosphorylation level of wild-type CFTR [23], but does not increase cAMP levels [17,18] or protein kinase A activity [23]. It can stimulate a basal CFTR activity [17,18] and intensifies cAMP-dependent CFTR channel activity [22,24], but cannot substitute for cAMP-dependent stimulation [19,24]. Finally, genistein delays de-activation of CFTR channel currents after removal of cAMP-dependent stimulation [19,24]. However, up to now no protein phosphatase has been shown to be inhibited by genistein. Furthermore, genistein can delay, but cannot prevent (like the protein phos-

Abbreviations used: CFTR, cystic fibrosis transmembrane conductance regulator; NBF, nucleotide-binding fold; CFTRΔF508, CFTR lacking Phe-508; pp[NH]pA, adenosine 5′-[β,γ-imido]triphosphate; MBP, maltose-binding protein; MBP–NBF-2, fusion protein comprising MBP and NBF-2; MBP–lacZ, fusion protein comprising MBP and the α-subunit of β-galactosidase; K_{ic} and K_{iu}, inhibition constants for competitive and uncompetitive inhibition respectively.

[1] To whom correspondence should be addressed (e-mail Randak@clinbio.med.uni-muenchen.de).

phatase inhibitor calyculin A), complete de-activation of the CFTR on removal of cAMP-dependent stimulation [24].

The most recent studies provide evidence for a direct action of genistein on the CFTR. First, it could be shown that, at all levels of CFTR phosphorylation, channel activity was greater in the presence of genistein than in its absence [22], which is not consistent with a mechanism where the sole effect of genistein is to alter CFTR phosphorylation. Secondly, various attempts to disrupt membrane-associated networks of protein kinase A and phosphatases, as well as of tyrosine kinases and phosphatases, failed to abolish genistein's effect on CFTR [25–27]. Analysis of the effects of genistein on the single-channel characteristics of CFTR revealed an increase in the mean open burst time [22,26,27]. Genistein cannot substitute for hydrolysable nucleotides, but requires the presence of hydrolysable ATP [25,27] or GTP [26]. Since genistein has been shown to act on ATP-binding sites [15], and since its effect on CFTR is similar to the consequences of CFTR mutations that are thought to prevent ATP hydrolysis at NBF-2 but not at NBF-1 [7,8], or to the effect of non-hydrolysable ATP analogues, such as adenosine 5′-[β,γ-imido]triphosphate (pp[NH]pA), that are also thought to lock CFTR channels open by interfering with ATP hydrolysis at NBF-2 [7,28], more detailed studies of the interaction of genistein with NBF-2 should provide mechanistic information on how genistein acts on CFTR.

The investigations described in the present paper have focused on a fusion protein (MBP–NBF-2) comprising NBF-2 and maltose-binding protein (MBP) that was originally overexpressed in *Escherichia coli* and purified in our laboratory [12]. We present kinetic data showing that the ATPase, GTPase and adenylate kinase activities of NBF-2 within the MBP–NBF-2 fusion protein [12] are readily inhibited by genistein in a partial non-competitive manner. Compelling evidence is provided that genistein interacts directly with NBF-2 within the fusion protein and that it interferes with pp[NH]pA binding. Thus the present study shows, for the first time, that genistein can interact directly with a CFTR domain.

EXPERIMENTAL

Reagents and enzymes

Genistein, daidzein, quercetin, DMSO and the various alcohols used were purchased from Sigma, except for ethanol, which was from Merck. The isoflavonoids were stored as 100 mM stock solutions in DMSO at −20 °C. Nucleotides, NADH and phosphoenolpyruvate were obtained from Boehringer Mannheim. pp[NH]pA was from Sigma. Pyruvate kinase, lactic dehydrogenase and adenylate kinase (from hog muscle) were from Boehringer Mannheim. (Na^+,K^+)-ATPase (from dog kidney) was purchased from Sigma.

Overexpression and purification of the MBP–NBF-2 fusion protein

Methodology has been described previously [12]. The CFTR cDNA sequence from base 3754 to base 4331 [1], coding for the CFTR protein sequence from Gly-1208 to Leu-1399 (numbering according to [1]), enclosing the whole predicted NBF-2, was introduced between the *Eco*RI and *Pst*I sites of the expression vector pMAL®-c2 (New England Biolabs®) in-frame with the coding sequence for MBP. The > 95 % pure MBP–NBF-2 fusion protein has been characterized chemically and functionally [12]. The protein employed in the studies reported here was from the same preparation and was stored at −80 °C in 50 mM Tris/HCl, pH 7.5.

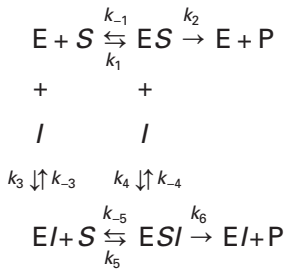

Scheme 1 Analysis of reversible, non-linear inhibition

k_1, k_{-1}, k_2, k_3, k_{-3}, k_4, k_{-4}, k_5, k_{-5} and k_6 are rate constants, E is free functional active enzyme, S is substrate, I is inhibitor and P is product.

Assays of enzymic activities

The assays were performed exactly as described previously [12]. ATPase activity was measured continuously at 25 °C by monitoring the decrease in absorption of NADH at 340 nm caused by the formation of ADP coupled to the pyruvate kinase and lactic dehydrogenase reactions. For this purpose the indicated amount of ATP and 2 μM MBP–NBF-2 were incubated together with 3 mM phosphoenolpyruvate, 0.27 mM NADH, 6.5 mM magnesium acetate, 34 mM KCl, 4.17 μg (1.9 units) of lactic dehydrogenase and 12.5 μg (1.9 units) of pyruvate kinase in 50 mM Tris/HCl, pH 7.5, in a total volume of 360 μl. GTPase activity was measured in exactly the same way, except that GTP was used as substrate instead of ATP. To measure adenylate kinase activity, 1 mM AMP was added to the buffer. We have previously demonstrated that, under these conditions, MBP–NBF-2 functions almost exclusively as an adenylate kinase, with negligible phosphate release [12]. At the end of each reaction, the addition of 0.5 mM ADP or GDP respectively verified that the assay would have measured the nascent product. Absorption was monitored using an Ultrospec II (LKB Biochrom) spectrophotometer.

CD spectroscopy

CD spectra (195–250 nm) were measured at 25 °C in an Auto-Dichrograph Mark IV (Jobin Yvon Division d'Instruments S.A.) spectropolarimeter which was calibrated at regular intervals with a standard solution of D(+)-10-camphorsulphonic acid and with isoandrosterone. Spectra were measured in steps of 0.1 nm, with a response time of 1 s and with the indicated protein concentrations, buffer compositions and path lengths. Each spectrum was the smoothed average of ten separate scans.

Fluorescence spectroscopy

All fluorescence measurements were carried out at 25 °C using a SPEX FluoroMax fluorimeter. Spectra were obtained with an increment of 0.5 nm and an integration time of 1 s. Without using a polarizer, the band pass for excitation and emission was 4.25 nm. With the polarizer installed, the band pass had to be increased to 10 nm (excitation) and 15 nm (emission). Excitation spectra of genistein were recorded at 480 nm emission. To measure emission spectra, genistein samples were excited at 325 nm. Spectra of samples containing MBP–NBF-2 or MBP–lacZ (a fusion protein comprising MBP and the α-subunit of β-galactosidase) were recorded as horizontally polarized emission after vertically polarized excitation, in order to minimize effects of light scattering [29] that might occur as a consequence of

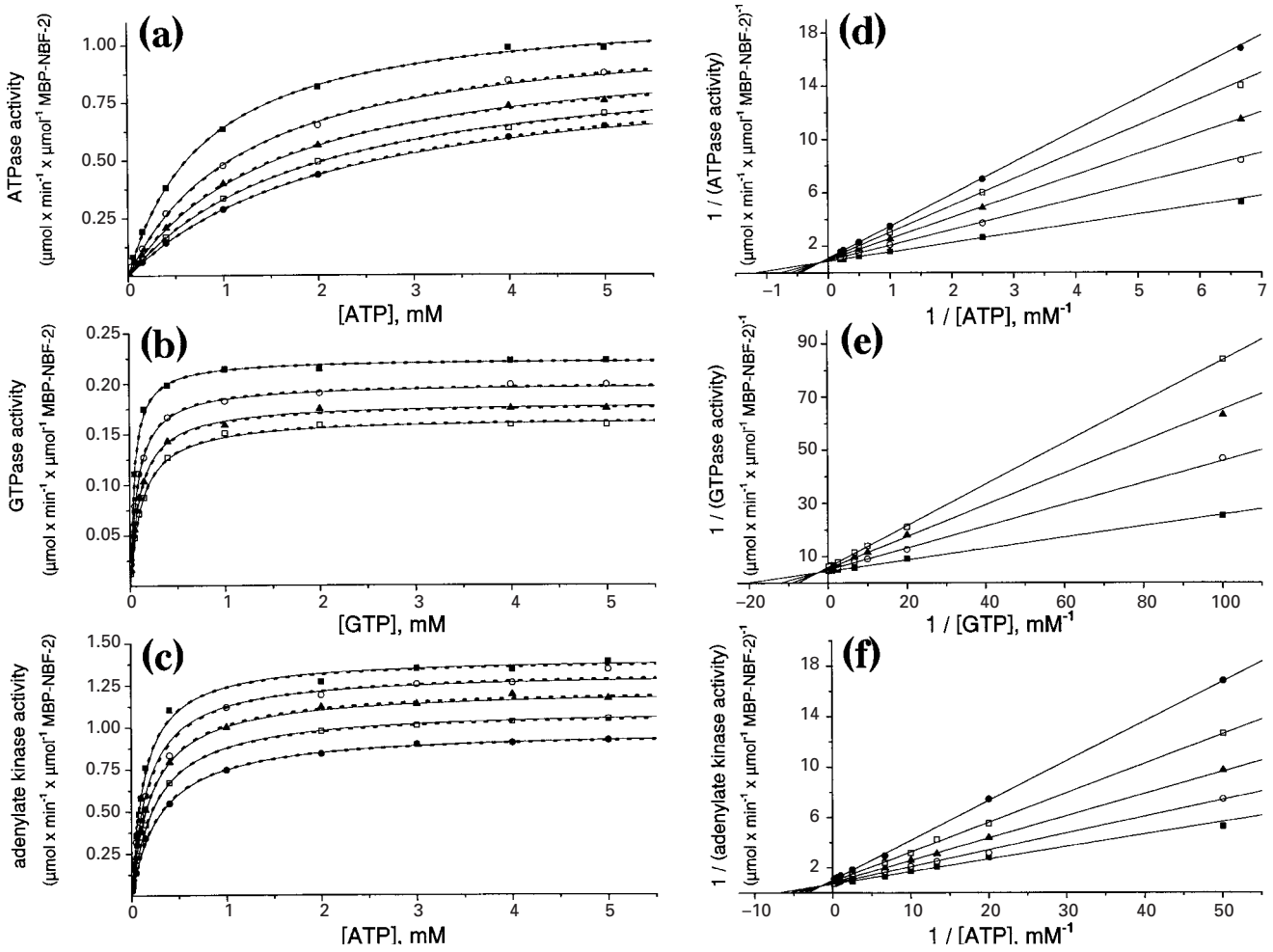

Figure 1 Effects of genistein on the initial rate kinetics of the ATPase (a, d), GTPase (b, e) and adenylate kinase (c, f) activities of MBP–NBF-2

(**a**)–(**c**) The ATPase (**a**), GTPase (**b**) and adenylate kinase (**c**) activities of MBP–NBF-2 are plotted as a function of substrate (ATP or GTP) concentration at genistein concentrations of (from top to bottom): 0 μM (■), 20 μM (○), 50 μM (▲), 100 μM (□) and 200 μM (●). Adenylate kinase activity (**c**) is plotted as a function of the ATP concentration, and was measured in the presence of a practically saturating concentration of AMP (1 mM), which causes MBP–NBF-2 to function almost exclusively as an adenylate kinase [12]. Solid lines represent the results of the non-linear least squares global fit to eqn. (1). Broken lines are the result of fitting the set of data obtained at the same genistein concentration to the equation $v = V_{max}(app) \cdot [S]/(K_m(app) + [S])$, which describes the dependence of reaction velocity (v) on the concentration of the substrate, S, which is ATP (**a**, **c**) or GTP (**b**). $K_m(app)$ and $V_{max}(app)$ represent the apparent K_m and the apparent V_{max} in the presence of a certain concentration of genistein. (**d**)–(**f**) Lineweaver–Burk plots. The data and solid lines of (**a**), (**b**) and (**c**) are drawn as double-reciprocal plots. The intersection of the lines in the Lineweaver–Burk plots with the ordinate for an individual concentration of the inhibitor genistein ([I]) is given by the term $(1 + [I]/K_{iu})/(V_{max} + V_{ESI}[I]/K_{iu})$, and that with the abscissa by the term $-(1 + [I]/K_{iu})/[K_m(1 + [I]/K_{ic})]$. All data points depicted are representative of two to six individual experiments.

aggregate formation, as has been described for a fusion protein comprising MBP and NBF-1 of CFTR [30].

Analytical treatment of inhibition

A general model to analyse reversible, non-linear inhibition, originally described by Botts and Morales [31], was employed to fit the kinetic data (see Scheme 1). Assuming that all steps up to product formation are fast relative to k_2 and k_6, and therefore that E, EI, ES and ESI are in equilibrium, the velocity ($v = d[P]/dt = k_2[ES] + k_6[ESI]$) of product formation is given by the following equation:

$$v = \frac{\left(V_{max} + \frac{V_{ESI}[I]}{K_{iu}}\right)[S]}{K_m\left(1 + \frac{[I]}{K_{ic}}\right) + \left(1 + \frac{[I]}{K_{iu}}\right)[S]} \quad (1)$$

K_{ic} and K_{iu} are the inhibition constants for competitive and uncompetitive inhibition respectively. The parameters of eqn. (1) are defined as follows (where $[E]_0$ is the concentration of the functional active enzyme initially added to the system):

$$V_{max} = k_2[E]_0 \quad (2)$$

$$V_{ESI} = k_6[E]_0 \quad (3)$$

$$K_m = (k_{-1} + k_2)/k_1 \quad (4)$$

$$K_{ic} = k_{-3}/k_3 = [E][I]/[EI] \quad (5)$$

$$K_{iu} = k_{-4}/k_4 = [ES][I]/[ESI] \quad (6)$$

Non-linear regression analysis

The parameters defined in eqns. (2)–(6) and their standard errors were obtained as a result of non-linear regression fitting using the

Marquardt–Levenberg algorithm [32] with the SigmaStat® statistical software (SPSS ASC GmbH, Erkrath, Germany).

RESULTS

Because of their very poor solubility in aqueous solution, genistein and the related compounds used in these investigations were dissolved in DMSO. Control experiments with DMSO alone added to a system of MBP–NBF-2 and the components of the employed enzymic ADP/GDP detection assay indicated that a concentration of 5% (v/v) DMSO reduced the rate of NADH decrease by 15%; 10% and 20% (v/v) DMSO strongly reduced the detected enzymic activities of MBP–NBF-2 by 45% and 70% respectively. DMSO concentrations above 20% (v/v) significantly inhibited the coupled pyruvate kinase/lactic dehydrogenase system itself. In our studies, we therefore used 1.5% (v/v) DMSO, which was shown to keep up to 200 μM genistein in solution, but did not measurably affect the three enzymic activities of MBP–NBF-2.

At a constant DMSO concentration of 1.5% (v/v), up to 200 μM genistein affected neither the coupled enzymic ADP/GDP detection assay itself nor the activity of (Na^+,K^+)-ATPase (from dog kidney) or adenylate kinase from hog muscle (results not shown). In contrast, genistein significantly inhibited the three enzymic activities of MBP–NBF-2. Velocities for each individual enzymic activity were measured at various substrate (ATP or GTP) and genistein concentrations (Figure 1). At each genistein concentration, typical Michaelis–Menten plots (Figures 1a–1c; broken lines) were obtained when activity was plotted against substrate concentration, resulting in the apparent K_m and V_{max} values given in Table 1. Genistein induced both an increase in the apparent K_m and a decrease in V_{max} for all three enzymic activities. For this reason neither a competitive nor a non-competitive mechanism alone could fully explain the observed inhibition. Therefore a general model of reversible inhibition (see the Experimental section) was used, and a global fit to eqn. (1) was performed. The results are given in Table 2 and illustrated in Figure 1 (solid lines). Since, for all three enzymic activities, the rate of substrate turnover did not decrease to zero at approximately saturating genistein concentrations (Figure 2), the inhibition could be described as partial non-competitive. As the relationship $K_{ic} < K_{iu}$ was found to be valid for all three enzymic functions, the mechanism could be further specified as mixed inhibition in which binding of the substrate (ATP or GTP) interferes with binding of the inhibitor genistein, and vice versa. This type of inhibition is reflected by the common point of intersection of the fitted lines in the Lineweaver–Burk plots of Figures 1(d)–1(f) located in the second quadrant.

Table 2 Kinetic constants for the inhibition of MBP–NBF-2 enzymic activities by genistein and related isoflavonoids

The enzymic activities were measured at 25 °C for between eight and ten ATP or GTP concentrations, and at genistein concentrations of 0, 20, 50, 100, 125 and 200 μM, or at daidzein or quercetin concentrations of 0, 20 and 50 μM. Higher concentrations of daidzein and quercetin were not soluble in 1.5% (v/v) DMSO. The kinetic parameters were determined by performing global fits to eqn. (1) with no weighting. The K_m and K_{ic} values marked with * were obtained as the best-fit values using the equation $v = V_{max} \cdot [S]/\{K_m \cdot (1 + [I]/K_{ic}) + [S]\}$ for competitive inhibition, where the substrate, S, is ATP or GTP, and the inhibitor, I, is quercetin. v is the reaction velocity, measured as a function of both [S] and [I]. The MBP–NBF-2 adenylate kinase kinetics were described for ATP as substrate at a practically saturating concentration of AMP (1 mM). The V_{max} values (in μmol·min^{-1}·μmol of MBP–NBF-2^{-1}) for the unimpeded reactions have been determined by this approach to be 1.16 ± 0.016 for ATPase activity, 0.22 ± 0.0012 for GTPase activity and 1.41 ± 0.011 for adenylate kinase activity. All values are means ± S.E.M.

	K_m (μM)	K_{ic} (μM)	K_{iu} (μM)	V_{ESI} / V_{max} (%)
ATPase				
Genistein	813 ± 37	20 ± 2	63 ± 7	71 ± 3
Daidzein	No inhibition detectable			
Quercetin	805 ± 62	25 ± 5	$> 10^4$	–
	805 ± 51*	25 ± 2*	–	
GTPase				
Genistein	47 ± 2	15 ± 1	54 ± 5	60 ± 2
Daidzein	No inhibition detectable			
Quercetin	48 ± 13	11 ± 7	$> 10^4$	–
	48 ± 11*	11 ± 5*	–	
Adenylate kinase				
Genistein	139 ± 5	46 ± 5	142 ± 19	48 ± 3
Daidzein	No inhibition detectable			
Quercetin	183 ± 11	17 ± 5	40 ± 14	57 ± 7

The unimpeded MBP–NBF-2 ATPase activity was characterized in this study by a V_{max} of 1.16 μmol·min^{-1}·μmol of MBP–NBF-2^{-1} and a K_m of about 800 μM. Both values are higher than those we have previously reported for the same MBP–NBF-2 preparation [12], in contrast with the reproducible K_m and V_{max} values for the MBP–NBF-2 GTPase and adenylate kinase activities. The reason for this is that, in our earlier studies, substrate (ATP) concentrations up to only 1 mM were assayed. In the subsequent, more detailed, investigations reported here, we had to recognize that MBP–NBF-2 activity still increased significantly at ATP concentrations above 1 mM, resulting in the higher V_{max} and K_m values. Thus millimolar concentrations of ATP are required to achieve maximum ATPase activity.

The K_m for the GTPase activity was found to be significantly lower (about 20 times) than that for the ATPase, while the V_{max}

Table 1 Effects of genistein on K_m and V_{max} values of the enzymic activities of MBP–NBF-2

Apparent V_{max} values are given in units of μmol·min^{-1}·μmol of MBP–NBF-2^{-1}. Apparent K_m values were obtained as best-fit values using the equation $v = V_{max} \cdot [S]/(K_m + [S])$, where v is the reaction velocity at a certain concentration of the inhibitor genistein, measured as a function of the concentration of the substrate S (ATP or GTP). Results are means ± S.E.M.

[Genistein] (μM)	ATPase		GTPase		Adenylate kinase	
	K_m (μM)	V_{max}	K_m (μM)	V_{max}	K_m (ATP) (μM)	V_{max}
0	808 ± 40	1.158 ± 0.022	48 ± 2	0.223 ± 0.002	134 ± 7	1.403 ± 0.016
20	1294 ± 159	1.099 ± 0.047	81 ± 3	0.200 ± 0.001	187 ± 12	1.330 ± 0.019
50	1510 ± 49	0.992 ± 0.012	109 ± 4	0.180 ± 0.001	215 ± 5	1.229 ± 0.006
100	1854 ± 85	0.946 ± 0.017	129 ± 5	0.166 ± 0.002	251 ± 4	1.097 ± 0.004
200	2249 ± 27	0.931 ± 0.005	–	–	299 ± 9	0.974 ± 0.006

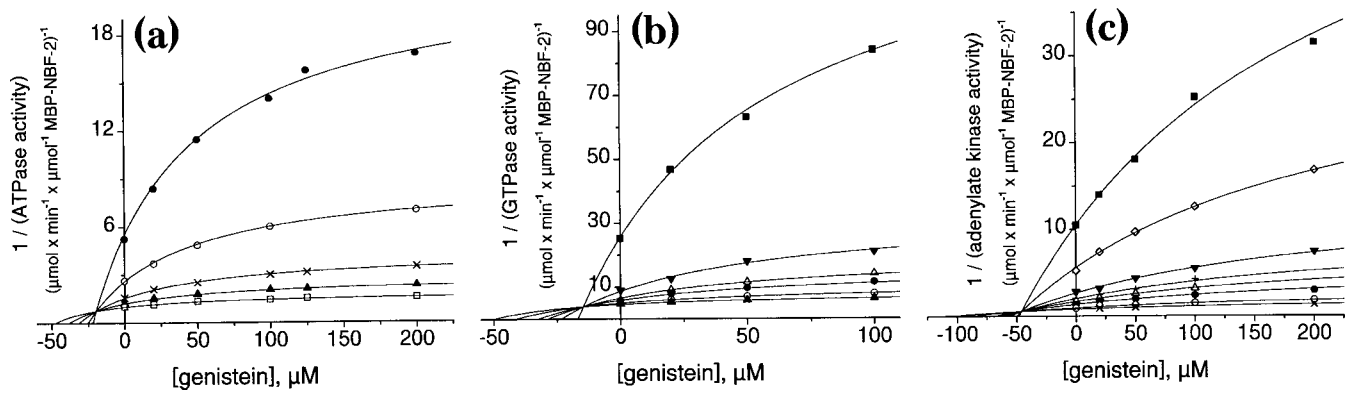

Figure 2 Partial inhibition of the enzymic activities of MBP–NBF-2 by genistein

Shown are Dixon plots [50] of the data of Figure 1 for inhibition by genistein of the ATPase (**a**), GTPase (**b**) and adenylate kinase (**c**) activities of MBP–NBF-2 at 10 μM (■), 20 μM (◇), 50 μM (▼), 75 μM (+), 100 μM (△), 150 μM (●), 400 μM (○), 1 mM (×), 2 mM (▲) and 5 mM (□) ATP (**a**, **c**) or GTP (**b**). The plots are not linear, but are curved and approach a horizontal asymptote at saturating genistein concentrations, indicating that the rate of substrate turnover does not decrease to zero after genistein has bound to MBP–NBF-2.

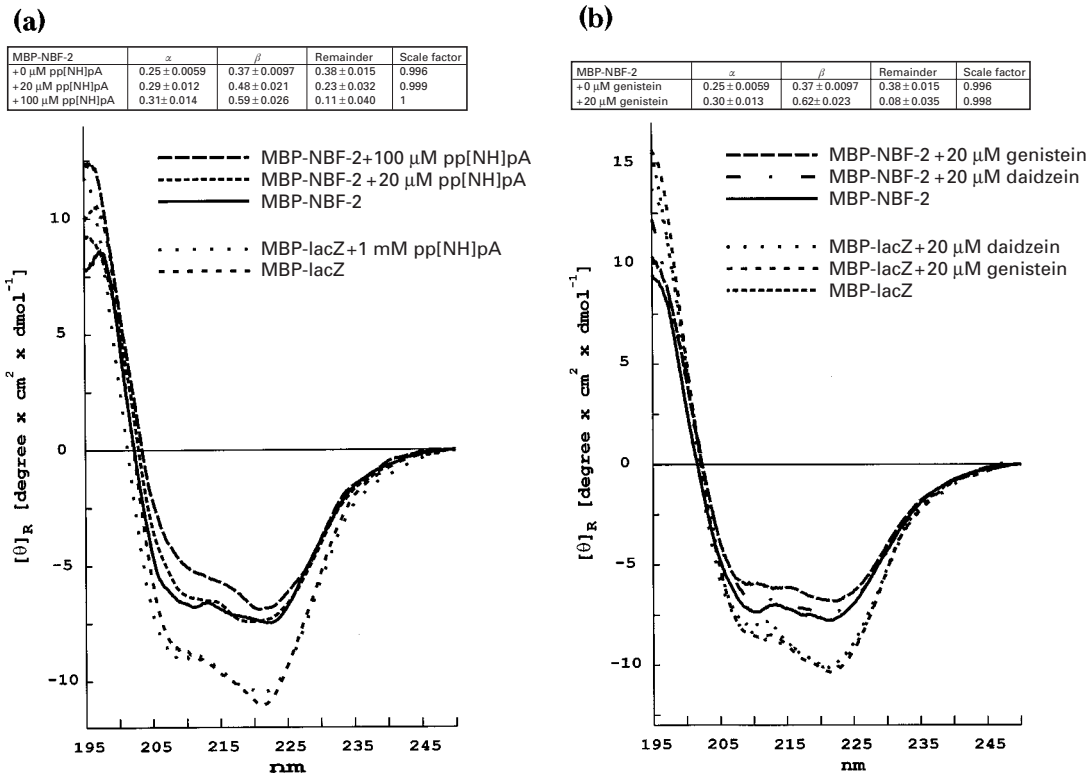

Figure 3 Influence of pp[NH]pA and isoflavonoids on CD spectra of MBP–NBF-2 and MBP–lacZ

(**a**) CD spectra of MBP–NBF-2 and MBP–lacZ (as a control) in the presence and absence of pp[NH]pA. Samples contained 0.115 mg/ml MBP–NBF-2 or 0.108 mg/ml MBP–lacZ in a buffer of 50 mM Tris/HCl, pH 7.5, and the indicated amount of pp[NH]pA, and were measured as described in the Experimental section with a path length of 1 mm. (**b**) CD spectra of MBP–NBF-2 and MBP–lacZ in the presence and absence of genistein or daidzein. Samples contained 1.15 mg/ml MBP–NBF-2 or 1.08 mg/ml MBP–lacZ in a buffer of 50 mM Tris/HCl, pH 7.5, 0.14% DMSO and 20 μM genistein or daidzein, and were measured with a path length of 0.1 mm. The spectrum of the buffer was subtracted from the particular protein spectrum in each case. The tables above the spectra give predicted secondary structures (means ± S.E.M.; total = 1.0) obtained from deconvolution CD spectra using the CONTIN FIT program [39].

of the unimpeded GTPase was about five times lower than that of the ATPase. Thus the affinity of MBP–NBF-2 for GTP seems to be higher than that for ATP, an observation that has been made previously in studies investigating the binding of GTP to NBF-2 fused to glutathione S-transferase [11]. It is noteworthy that the K_m for the adenylate kinase activity of the MBP–NBF-2–AMP complex with ATP as substrate was also lower than that for the ATPase activity, i.e. with ATP as substrate in the absence of AMP. Thus an increased affinity for ATP was observed after AMP binding.

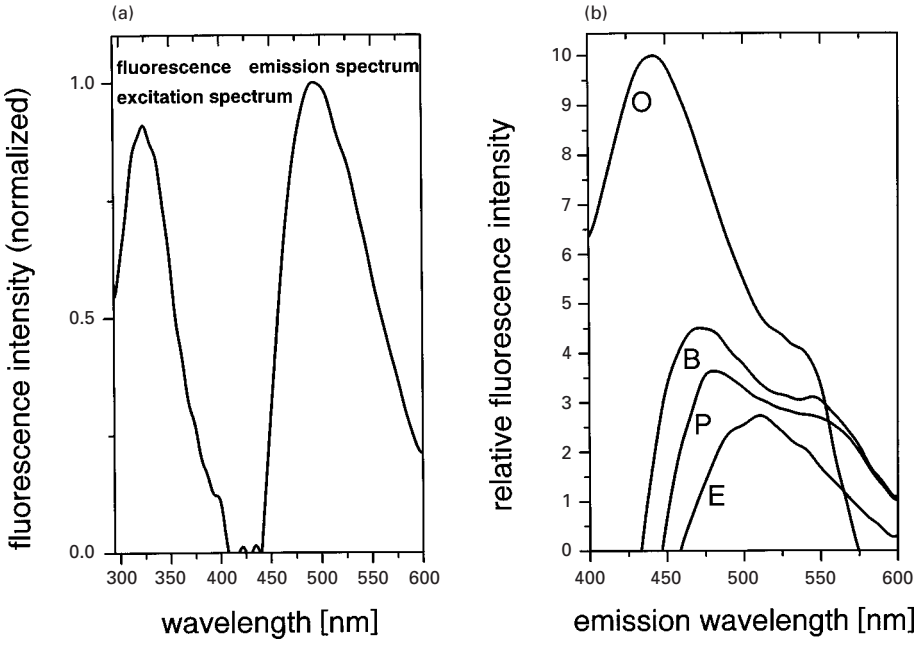

Figure 4 Fluorescence excitation and emission spectra of genistein

(**a**) Excitation and emission spectra of genistein in buffer containing 6.5 mM magnesium acetate, 34 mM KCl, 1.5% (v/v) DMSO and 50 mM Tris/HCl, pH 7.5. The depicted spectra are the normalized representatives of recording spectra for three different genistein concentrations (50, 100 and 200 μM). (**b**) Fluorescence emission spectra of genistein in various alcohols: ethanol (E), propan-1-ol (P), butan-1-ol (B) and octan-1-ol (O). Each spectrum in (**b**) was recorded twice and for two different genistein concentrations (100 and 200 μM). All spectra were obtained without using a polarizer. In all cases, the spectrum of the solvent was measured separately and subtracted from the particular genistein spectrum.

The binding of genistein to MBP–NBF-2 reduced the V_{max} values by 29% (ATPase), 40% (GTPase) and 52% (adenylate kinase). The effect of genistein at low substrate concentrations, expressed as the ratio of rates at saturating and zero genistein concentrations, is given by $(V_{ESI} \cdot K_{ic})/(V_{max} \cdot K_{iu})$, which is, in an equilibrium binding model, the ratio of V_{max}/K_m at infinite and zero inhibitor concentrations. According to the parameters given in Table 2, genistein lowers V_{max}/K_m by 77% (ATPase), 83% (GTPase) and 85% (adenylate kinase).

The effects of genistein on the kinetics of MBP–NBF-2 were compared with those of closely related compounds. Daidzein (4′,7-dihydroxyisoflavone), which differs from genistein only in the lack of a hydroxy group substitution at C-5, did not influence any activity of MBP–NBF-2 at concentrations up to 50 μM. Higher concentrations of daidzein could not be tested due to lack of solubility in 1.5% (v/v) DMSO. Quercetin (3,3′,4′,5,7-pentahydroxyflavone) displayed a competitive type of inhibition of the ATPase and GTPase activities of MBP–NBF-2. The latter findings were not unexpected, since competition by quercetin with the substrate ATP or GTP has been shown for several enzymes [33–36]. In addition, the crystal structure of the Src-family tyrosine kinase Hck has recently been determined in complex both with quercetin and with pp[NH]pA [37]. According to this structure, quercetin, which is significantly smaller than the pp[NH]pA molecule, binds to that portion of the ATP-binding pocket that interacts with the adenosine group. Similar behaviour in association with MBP–NBF-2 would explain the (with regard to substrate ATP) uncompetitive component of inhibition of MBP–NBF-2 adenylate kinase activity on replacement of bound AMP with quercetin.

Quercetin did not impair the enzymic assay system employed to detect nascent ADP or GDP. At even the highest quercetin concentration used (50 μM; 17 μg/ml), the addition of ADP or GDP resulted in an immediate, equimolar decrease in the concentration of NADH without any detectable delay. In a study by Grisolia and co-workers [38], inhibitory effects of quercetin on pyruvate kinase and, in particular, lactic dehydrogenase activities were observed. The lack of any observed susceptibility of our assay system to the amounts of quercetin employed can be explained by our much higher enzyme/quercetin concentration ratios, which were 3.5-fold higher for pyruvate kinase and 145-fold higher for lactic dehydrogenase, as well as by the huge excess of pyruvate kinase and lactic dehydrogenase activities that distinguishes the enzymic assay used in the studies reported here.

In order to demonstrate direct binding of genistein to the NBF-2 part of MBP–NBF-2, as suggested by the kinetic model, we studied the influence of complex-formation on the biophysical properties of both the protein and the ligand. Since neither the three-dimensional structures of CFTR or NBF-2 nor methods to crystallize either of those proteins are known, we investigated whether changes in the CD spectra of MBP–NBF-2 could be induced by genistein. As depicted in Figure 3(a) and 3(b), we compared the effects of genistein, daidzein and pp[NH]pA on the CD spectra of MBP–NBF-2 and MBP–lacZ (expressed and purified under identical conditions as MBP–NBF-2). In the presence of pp[NH]pA or genistein, the spectra of MBP–NBF-2 shifted to spectra of a more ordered form, which can be explained by a decrease in the fraction of 'remainder class' structure [39], i.e. turns and random coils, mainly in favour of an increase in β-stranded structure. No significant alteration of the CD spectrum was noted in the presence of daidzein. Neither of the substances employed had an influence on the CD spectrum of MBP–lacZ. These results demonstrate that genistein, but not daidzein, generates similar structural changes in NBF-2 as does the ATP analogue pp[NH]pA, a known ligand of NBF-2, and that complex-formation induces a more ordered structure.

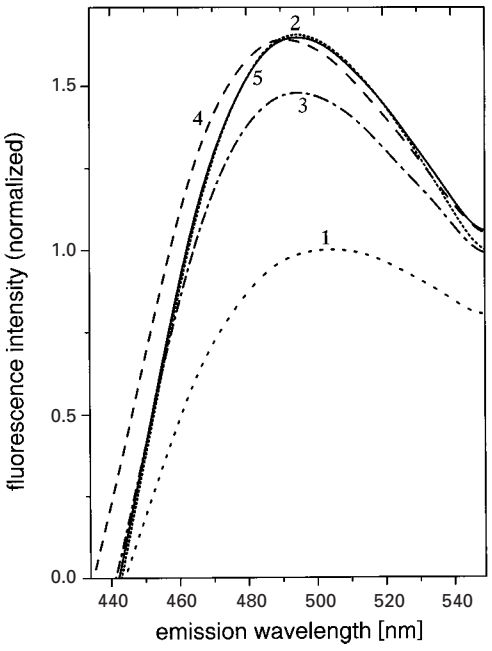

Figure 5 Fluorescence emission spectra of genistein in the presence or absence of MBP–NBF-2 and nucleotides

All samples contained 200 μM genistein in a buffer of 6.5 mM magnesium acetate, 34 mM KCl, 1.5% (v/v) DMSO and 50 mM Tris/HCl, pH 7.5. After vertically polarized excitation (325 nm), emission spectra were recorded through a horizontally oriented polarizer, which accounts for the 12 nm shift to longer wavelengths of the emission spectrum of genistein without MBP–NBF-2 (spectrum 1) in comparison to Figure 4(a). Spectra 2–5 were obtained from samples of 200 μM genistein and 2 μM MBP–NBF-2 (spectrum 2, dotted line), 2 μM MBP–NBF-2 and 100 μM pp[NH]pA (spectrum 3), 2 μM MBP–NBF-2 and 300 μM AMP (spectrum 4) or 2 μM MBP–NBF-2 and 300 μM GMP (spectrum 5, solid line) added to the buffer. In all cases the spectrum of the buffer (including protein and nucleotides as indicated) was measured separately and subtracted from the particular genistein spectrum. Spectra representative of those from five individual experiments are presented.

In order to demonstrate complex-formation between genistein and MBP–NBF-2 by monitoring changes in signals radiated from genistein, the following set of experiments was designed. As genistein possesses a system of delocalized electrons, as well as the possibility of forming mesomeric states via hydroxy-group substitutions at C-5, C-7 and C-4′ of the aromatic rings, it should be possible to use this compound as an intrinsic fluorophore that is sensitive to the chemical and physical properties of its solvents. Therefore the fluorescence properties of genistein were characterized (Figure 4). In Tris/HCl, pH 7.5, genistein has an absorption maximum at 325 nm that coincides with the maximum of the excitation spectrum. The wavelength distribution of the emission has a maximum at 492 nm (Figure 4a). Figure 4(b) shows the emission spectra of genistein in monohydroxy alcohols of increasing length. As the solvent polarity decreases, the quantum yield increases and the emission maximum shifts to shorter wavelengths. In octan-1-ol the emission maximum of genistein is at 442 nm. As illustrated in Figure 5, addition of MBP–NBF-2 induced a significant increase in the fluorescence of genistein, as well as a blue shift of 10 nm in the maximum of the emission spectrum. These findings indicate a solvent change towards a less polar environment, and are consistent with the binding of genistein to a non-polar region within the NBF-2 part of MBP–NBF-2, as a comparable effect could not be detected upon mixing genistein and MBP–lacZ (results not shown). Addition of an excess of pp[NH]pA partially eliminated this fluorescence enhancement and blue shift, indicating a reduced affinity of genistein for the complex of MBP–NBF-2 and pp[NH]pA. Unlike pp[NH]pA, addition of AMP caused a further 4 nm blue shift of the emission maximum. Such a blue shift is generally attributed to reduced solvent relaxation, i.e. a reduced ability of solvent molecules to reorient during the lifetime of the excited state of the fluorophore [29]. In contrast with the effects of AMP and pp[NH]pA, addition of GMP changed neither the fluorescence enhancement nor the wavelength distribution of the emitted light (Figure 5).

DISCUSSION

This study describes a direct interaction of genistein with the human CFTR NBF-2 domain of a recombinant MBP–NBF-2 fusion protein which results in inhibition of its three enzymic activities, i.e. ATPase, GTPase and adenylate kinase. The primary assumption on which the significance of the study rests is that the physiologically relevant functions of NBF-2 contained in endogenous CFTR resemble those of MBP–NBF-2, which is most probably true for the observed ATPase activity of MBP–NBF-2. ATP hydrolysis by the CFTR is in accordance with a generally accepted model of channel regulation that has been further supported by the demonstration of an ATPase activity of purified CFTR expressed in Sf9 insect cells [40]. Several groups have obtained evidence, based on electrophysiological studies with wild-type CFTR and CFTRs bearing amino acid substitutions in conserved regions of both NBFs, that ATP hydrolysis at NBF-2 induces channel closing, and that any inhibition of this ATP hydrolysis causes prolonged channel opening [7–9]. The observed K_m value for the ATPase activity of the recombinant NBF-2 of about 800 μM would predict a high level of activity at intracellular physiological levels of ATP [41]. The observations that CFTR could be activated with slightly reduced efficiency when ATP was replaced by GTP as the hydrolysable nucleotide [5,26], and that this replacement did not impair the ability of genistein to stimulate CFTR activity [26], would suggest that the NBF-2 domain of endogenous CFTR can hydrolyse GTP instead of ATP, similar to isolated NBF-2 fused to MBP. Again, the K_m of about 40 μM for the GTPase activity of MBP–NBF-2 would predict a high level of activity at intracellular physiological levels of GTP, which are assumed to be of the order of 1 mM [42]. Although further evidence that GTP hydrolysis by NBF-2 might be of physiological relevance has been provided by a study that suggested for NBF-2 a structure and function analogous to those of GTP-binding and -hydrolysing proteins [9], a physiological role for GTP hydrolysis by NBF-2 in a model of CFTR channel regulation has not yet been established. This is also the case for the adenylate kinase activity of recombinant NBF-2. It has been observed that, in the presence of ATP, AMP strongly inhibited CFTR Cl^- conductance in the sweat duct, and that in the same system ADP activated Cl^- conductance, which could be blocked by the adenylate kinase inhibitor diadenosine tetraphosphate [43]. This is, to our knowledge, the only evidence so far that an adenylate kinase activity may be associated with endogenous CFTR.

The observed inhibition of the ATPase activity of MBP–NBF-2 by genistein raises the question of whether inhibition of ATP hydrolysis at NBF-2 of the intact CFTR contributes to the observed reversible effect of genistein to increase the mean open burst time [22,26,27] of wild-type CFTR and of CFTRΔF508 [22]. In a recent study by Weinreich and co-workers [25] using excised patches from *Xenopus* oocytes expressing CFTR, genistein could not activate CFTR currents in the absence of ATP. At a constant MgATP concentration of 500 μM (the only

ATP concentration that was investigated), the genistein concentration for half-maximal stimulation of CFTR Cl^- currents was around 80 μM (84 $\pm$ 36 μM [25]). According to the kinetic data obtained in the present study, 50 % inhibition of MBP–NBF-2 ATPase activity at 500 μM ATP was achieved with 68 μM genistein. Together with the above-cited evidence proposing that ATP hydrolysis at NBF-2 induces channel closing, this close correlation strongly suggests that genistein causes prolonged channel opening by binding to NBF-2 and inhibiting ATP hydrolysis. Of course, it is possible that genistein might also bind to other parts of CFTR, e.g. NBF-1. Evidence for two-site binding was recently obtained in a study by Wang et al. [27], who observed an additional inhibitory effect of high genistein concentrations on CFTR chloride currents and proposed the presence of a second, low-affinity site that should reduce the opening rate. However, at the same high genistein concentrations, other groups [25,26] did not observe this inhibitory effect. While it is generally accepted that NBF-1 plays an important role in activating CFTR chloride currents, it is still controversial as to whether ATP hydrolysis [5,7,9,28] or non-hydrolytic ATP binding at NBF-1 [43] is the significant event in the opening of phosphorylated CFTR. In addition, the functional properties of isolated NBF-1 domain proteins vary markedly between investigators, ranging from high-affinity ATP binding (K_d 2.2 μM) and no detectable hydrolytic activity [44] to low-affinity ATP binding (K_d 1.8 mM) and ATP hydrolysis [30,45]. Therefore the significance of a potentially detectable interaction of genistein with an isolated NBF-1 polypeptide for the regulation of intact CFTR is currently difficult to evaluate. Nevertheless, we conclude that inhibition of NBF-2 ATP hydrolysis is a major mechanism behind the genistein-dependent stimulation of CFTR chloride currents.

The kinetic data presented in this paper imply that genistein binds to a site in NBF-2 that is not identical with either nucleotide-binding pocket, otherwise the rate of substrate turnover would decrease to zero at saturating genistein concentrations. On the other hand, the relationship with the ATP/GTP-binding pocket must be close enough to account for the mutual interference of binding observed for genistein and ATP/GTP. Similar conclusions can be drawn from the fluorescence binding and competition studies: according to these results, genistein binds to a non-polar region of NBF-2, inducing fluorescence enhancement. This site must be closely related to the ATP-binding site, since an excess of pp[NH]pA partially reduced the enhanced fluorescence. AMP caused a blue shift of the emission spectrum of genistein bound to MBP–NBF-2, consistent with reduced solvent relaxation that would be explained by lowered mobility of the amino acid molecules that are in the immediate vicinity of the fluorophore. For adenylate kinases, induced-fit movements have been described [46] that are initiated by AMP binding and result in the closure of a hinged domain over the bound ATP molecule [47] and a reassembled active centre. We speculate that MBP–NBF-2 also undergoes conformational changes upon substrate binding, since AMP, but not GMP, which as a rule is not bound to the AMP site in the adenylate kinase family [13,48,49], induced the blue shift of the emission spectrum of bound genistein. We conclude from the occurrence of this blue shift that the amino acid residues surrounding the bound genistein have moved to a more rigid position as a consequence of a conformational change induced by AMP binding. Our kinetic studies also support a conformational change in MBP–NBF-2 after AMP binding, since the Michaelis constant for ATP as substrate was determined to be significantly lower in the presence of AMP. This observation requires a smaller rate constant k_{-1}, which describes the rate of dissociation of bound ATP from the complex with MBP–NBF-2. The latter would again be explained by a conformational change induced by AMP, leading to tighter binding of ATP.

In conclusion, this work provides the first biochemical evidence for an interaction between CFTR and genistein. Our observations demonstrate that genistein inhibits NBF-2 activity as the result of specific binding to this domain, and suggest a similar mechanism for the potent stimulation of CFTR and CFTRΔF508 currents by genistein. Thus this naturally occurring compound may prove useful in the treatment of patients with cystic fibrosis.

We thank L. Moroder (Max-Planck-Institut für Biochemie, Martinsried, Germany) for use of the CD spectropolarimeter, and E. Weyher-Stingl for technical assistance during CD measurements. C. R. is grateful to H.-B. Hadorn (Department of Pediatrics, Dr. von Haunersches Kinderspital, München) for supporting this work by partially releasing C. R. from his clinical duties. This work was supported by the Deutsche Forschungsgemeinschaft (Ra 682/3-2).

REFERENCES

1 Riordan, J. R., Rommens, J. M., Kerem, B., Alon, N., Rozmahel, R., Grzelczak, Z., Zielenski, J., Lok, S., Plavsic, N., Chou, J. L. et al. (1989) Science **245**, 1066–1073
2 Hyde, S. C., Emsley, P., Hartshorn, M. J., Mimmack, M. M., Gileadi, U., Pearce, S. R., Gallagher, M. P., Gill, D. R., Hubbard, R. E. and Higgins, C. F. (1990) Nature (London) **346**, 362–365
3 Manavalan, P., Dearborn, D. G., McPherson, J. M. and Smith, A. E. (1995) FEBS Lett. **366**, 87–91
4 Cheng, S. H., Rich, D. P., Marshall, J., Gregory, R. J., Welsh, M. J. and Smith, A. E. (1991) Cell **66**, 1027–1036
5 Anderson, M. P., Berger, H. A., Rich, D. P., Gregory, R. J., Smith, A. E. and Welsh, M. J. (1991) Cell **67**, 775–784
6 Anderson, M. P. and Welsh, M. J. (1992) Science **257**, 1701–1704
7 Carson, M. R., Travis, S. M. and Welsh, M. J. (1995) J. Biol. Chem. **270**, 1711–1717
8 Smit, L. S., Wilkinson, D. J., Mansoura, M. K., Collins, F. S. and Dawson, D. C. (1993) Proc. Natl. Acad. Sci. U.S.A. **90**, 9963–9967
9 Carson, M. R. and Welsh, M. J. (1995) Biophys. J. **69**, 2443–2448
10 Randak, C., Roscher, A. A., Hadorn, H. B., Assfalg-Machleidt, I., Auerswald, E. A. and Machleidt, W. (1995) FEBS Lett. **363**, 189–194
11 Randak, C., Neth, P., Auerswald, E. A., Assfalg-Machleidt, I., Roscher, A. A., Hadorn, H. B. and Machleidt, W. (1996) FEBS Lett. **398**, 97–100
12 Randak, C., Neth, P., Auerswald, E. A., Eckerskorn, C., Assfalg-Machleidt, I. and Machleidt, W. (1997) FEBS Lett. **410**, 180–186
13 Tomasselli, A. G. and Noda, L. H. (1980) Eur. J. Biochem. **103**, 481–491
14 Müller, C. W. and Schulz, G. E. (1992) J. Mol. Biol. **224**, 159–177
15 Akiyama, T., Ishida, J., Nakagawa, S., Ogawara, H., Watanabe, S., Itoh, N., Shibuya, M. and Fukami, Y. (1987) J. Biol. Chem. **262**, 5592–5595
16 Huang, J., Nasr, M., Kim, Y. and Matthews, H. R. (1992) J. Biol. Chem. **267**, 15511–15515
17 Illek, B., Fischer, H., Santos, G. F., Widdicombe, J. H., Machen, T. E. and Reenstra, W. W. (1995) Am. J. Physiol. **268**, C886–C893
18 Lehrich, R. W. and Forrest, Jr., J. N. (1995) Am. J. Physiol. **269**, F594–F600
19 Illek, B., Fischer, H. and Machen, T. E. (1996) Am. J. Physiol. **270**, C265–C275
20 Shuba, L. M., Asai, T., Pelzer, S. and McDonald, T. F. (1996) Br. J. Pharmacol. **119**, 335–345
21 Illek, B., Yankaskas, J. R. and Machen, T. E. (1997) Am. J. Physiol. **272**, L752–L761
22 Hwang, T. C., Wang, F., Yang, I. C. and Reenstra, W. W. (1997) Am. J. Physiol. **273**, C988–C998
23 Reenstra, W. W., Yurko-Mauro, K., Dam, A., Raman, S. and Shorten, S. (1996) Am. J. Physiol. **271**, C650–C657
24 Yang, I. C., Cheng, T. H., Wang, F., Price, E. M. and Hwang, T. C. (1997) Am. J. Physiol. **272**, C142–C155
25 Weinreich, F., Wood, P. G., Riordan, J. R. and Nagel, G. (1997) Pflügers Arch. **434**, 484–491
26 French, P. J., Bijman, J., Bot, A. G., Boomaars, W. E., Scholte, B. J. and de Jonge, H. R. (1997) Am. J. Physiol. **273**, C747–C753
27 Wang, F., Zeltwanger, S., Yang, I. C. H., Nairn, A. C. and Hwang, T. C. (1998) J. Gen. Physiol. **111**, 477–490
28 Hwang, T. C., Nagel, G., Nairn, A. C. and Gadsby, D. C. (1994) Proc. Natl. Acad. Sci. U.S.A. **91**, 4698–4702
29 Lakowicz, J. R. (1983) Principles of Fluorescence Spectroscopy, Plenum Press, New York
30 Ko, Y. H., Thomas, P. J., Delannoy, M. R. and Pedersen, P. L. (1993) J. Biol. Chem. **268**, 24330–24338

31 Botts, J. and Morales, M. (1953) Trans. Faraday Soc. **49**, 696–707
32 Marquardt, D. W. (1963) SIAM J. Appl. Math. **11**, 431–441
33 Horn, F., Gschwendt, M. and Marks, F. (1985) Eur. J. Biochem. **148**, 533–538
34 Cochet, C., Feige, J. J., Pirollet, F., Keramidas, M. and Chambaz, E. M. (1982) Biochem. Pharmacol. **31**, 1357–1361
35 Cochet, C. and Chambaz, E. M. (1986) Biochem. J. **237**, 25–31
36 McKenna, E., Smith, J. S., Coll, K. E., Mazack, E. K., Mayer, E. J., Antanavage, J., Wiedmann, R. T. and Johnson, Jr., R. G. (1996) J. Biol. Chem. **271**, 24517–24525
37 Sicheri, F., Moarefi, I. and Kuriyan, J. (1997) Nature (London) **385**, 602–609
38 Grisolia, S., Rubio, V., Feijoo, B. and Mendelson, J. (1975) Physiol. Chem. Phys. **7**, 473–475
39 Provencher, S. W. and Glockner, J. (1981) Biochemistry **20**, 33–37
40 Ramjeesingh, M., Li, C., Garami, E., Huan, L. J., Hewryk, M., Wang, Y., Galley, K. and Bear, C. E. (1997) Biochem. J. **327**, 17–21
41 Atkinson, D. E. (1977) Cellular Energy Metabolism and its Regulation, Academic Press, New York
42 Goody, R. S., Frech, M. and Wittinghofer, A. (1991) Trends Biochem. Sci. **16**, 327–328
43 Quinton, P. M. and Reddy, M. M. (1992) Nature (London) **360**, 79–81
44 Yike, I., Ye, J., Zhang, Y., Manavalan, P., Gerken, T. A. and Dearborn, D. G. (1996) Protein Sci. **5**, 89–97
45 Ko, Y. H. and Pedersen, P. L. (1995) J. Biol. Chem. **270**, 22093–22096
46 Schulz, G. E., Müller, C. W. and Diederichs, K. (1990) J. Mol. Biol. **213**, 627–630
47 Bilderback, T., Fulmer, T., Mantulin, W. W. and Glaser, M. (1996) Biochemistry **35**, 6100–6106
48 Müller-Dieckmann, H. J. and Schulz, G. E. (1995) J. Mol. Biol. **246**, 522–530
49 Ito, Y., Tomasselli, A. G. and Noda, L. H. (1980) Eur. J. Biochem. **105**, 85–92
50 Dixon, M. (1953) Biochem. J. **55**, 170–171

Received 11 November 1998/26 January 1999; accepted 11 March 1999